

# Anatomical Differences in the 3D Morphology of the Bones of the Foot and Ankle Between Female Patients with Progressive Collapsing Foot Deformity and Asymptomatic Controls

Takuma Miyamoto<sup>1,2</sup>, Rich Lisonbee<sup>1</sup>, Kassidy Knutson<sup>1</sup>, Hiroaki Kurokawa<sup>2</sup>, Akira Taniguchi<sup>2</sup>, Yasuhiro Tanaka<sup>2</sup>, Amy Lenz<sup>1</sup>, Andrew Anderson<sup>1</sup>

<sup>1</sup>University of Utah, UT, USA, <sup>2</sup>Nara Medical University, Nara, Japan

Email: [takuma.miyamoto@utah.edu](mailto:takuma.miyamoto@utah.edu)

**INTRODUCTION:** Progressive collapsing foot deformity (PCFD) represents a multifaceted three-dimensional condition of the foot and ankle. As part of previous research and in clinical practice, PCFD is typically evaluated through plain film x-rays and/or computed tomography (CT) images [1]. However, these measurements do not evaluate the morphology of the individual bones of the foot and ankle. Knowledge of these anatomical deformities could enhance diagnosis and treatment efforts for PCFD. Herein, we quantified anatomical variation and compared the shape of the individual bones of the foot and ankle using a 3D statistical shape model (SSM). Based on our clinical impressions, and after considering the results of several studies examining PCFD morphology, we hypothesized that the talus and calcaneus would exhibit the most substantial differences in bone shape between groups, with a “down-the-chain” impact focused through the medial-longitudinal arch of the foot.

**METHODS:** With IRB approval from both institutions, 3D bone reconstructions from clinical CT images of 23 female patients presenting with PCFD (age:  $65.1 \pm 7.1$ ) and 23 female asymptomatic individuals (age:  $46.7 \pm 19.2$ ) underwent simulated weight-bearing CT (SW-CT) (0.625 mm slice thickness, 512/512 matrix). For each participant, SW-CT images were auto-segmented to create 3D models of distal tibia, distal fibula, talus, calcaneus, navicular, cuboid, all cuneiforms, and all metatarsal bones, respectively (Disior 2.1, Bonelogic). Manual verification of bone models was performed using Mimics 22.0 (Materialise). Pre-processing of the 3D bone reconstructions included mirroring left bones to represent right bones, aligning and centering each bone (for each respective bone) using an iterative closest point algorithm. A single domain statistical shape model was performed for each bone, respectively, across all 46 participants to generate SSMs using ShapeWorks 6.4.1 (University of Utah). Procrustes scaling was used to account for size variation in the model population. 16 separate models were optimized for each bone/domain. A principal component analysis (PCA) was used to determine modes of variation as well as PCA component scores across both study groups for all 16 models. The PCA modes containing significant variation were determined using parallel analysis. Within significant PCA modes, PCA component scores were tested for normality using a Shapiro-Wilk test, then compared using the appropriate Mann-Whitney t-test (for normal) or Wilcoxon rank sum test (for not normal) to compare PCA scores between patients with PCFD and control participants within that mode identified by parallel analysis. PCA component score tests across modes for a specific domain were corrected using a Holm-Sidak correction to reduce the probability of type 1 error. For all statistical measures and comparisons an alpha value of 0.05 was used ( $p < 0.05$ ) (Figure 1).

**RESULTS:** Single domain SSM analysis of individuals presenting with PCFD exhibited several significant modes of variation across the various bones. Notably, Mode 3 for the fibula, capturing 7.0% of the explained variance, showed a reduction in the fibula tip as well as an increase in the anterior/posterior width of the talofibular articular facet in PCFD patients. Modes 1 and 2 (14.4% and 12.4% explained variance) demonstrated that the PCFD cohort presented with a decrease in the lateral and posterior processes of the talus, a shift of the talar head inferior and adductor, a thicker talar neck, and a reduced talar head. Mode 2 for the calcaneus (13.6 % explained variance) indicated a narrow posterior facet and an anteriorly shifted anterior-medial facet. Mode 3 for the navicular (11.4% explained variance) showed the navicular tuberosity was shifted towards the body, with medial-inferior defects in the articular surface of the navicular, along with a lateral shift of the navicular beak amongst PCFD patients. Finally, Mode 3 for the cuboid (8.0% explained variance) represented an increase in the prominence of the cuboid tuberosity and beak in patients (Figure 2).

**DISCUSSION:** This is the first paper to study using SSM to simultaneously analyze the 3D shape of bones from the tibia to the metatarsals in both PCFD and asymptomatic controls in females. In general, our hypothesis was confirmed. Notably, we found that patients with PCFD exhibited 3D differences in the shape of the distal fibula, talus, calcaneus, navicular, and cuboid. Differences were not significant in bones that were further down the chain, including the cuneiforms and metatarsals. Contrary to our hypothesis, the distal tibia was not significantly different between groups; we believe this is because the tibia, which is said to be associated with ankle joint valgus instability, is less associated with PCFD and more likely to be caused by hindfoot valgus instability. Collectively, our study highlights the complexity of the foot and ankle of individuals presenting with PCFD and the value in robust 3D analyses to evaluate PCFD. Still, we acknowledge the limitations of the study, including the inclusion of only females as well

as larger age differences between controls and patients. Future research will focus on expanding the SSM models described herein to include a broader spectrum of patients and control participants.

## CLINICAL RELEVANCE:

The SSM results presented herein could help in the diagnosis and treatment of PCFD by providing a thorough, 3D characterization of the deformities of the individual bones of the foot and ankle.

**REFERENCES:** [1] Lintz, F. et al. Foot Ankle Surg. 2022, [2] Broos, M. et al. Eur J Radiol. 2021

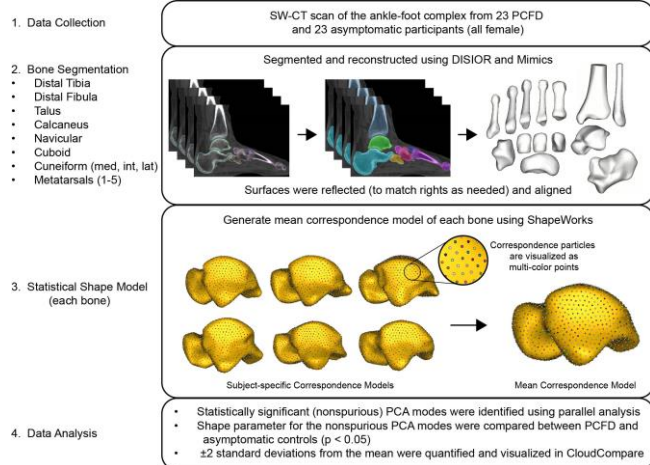


Figure 1: Computational workflow for this study

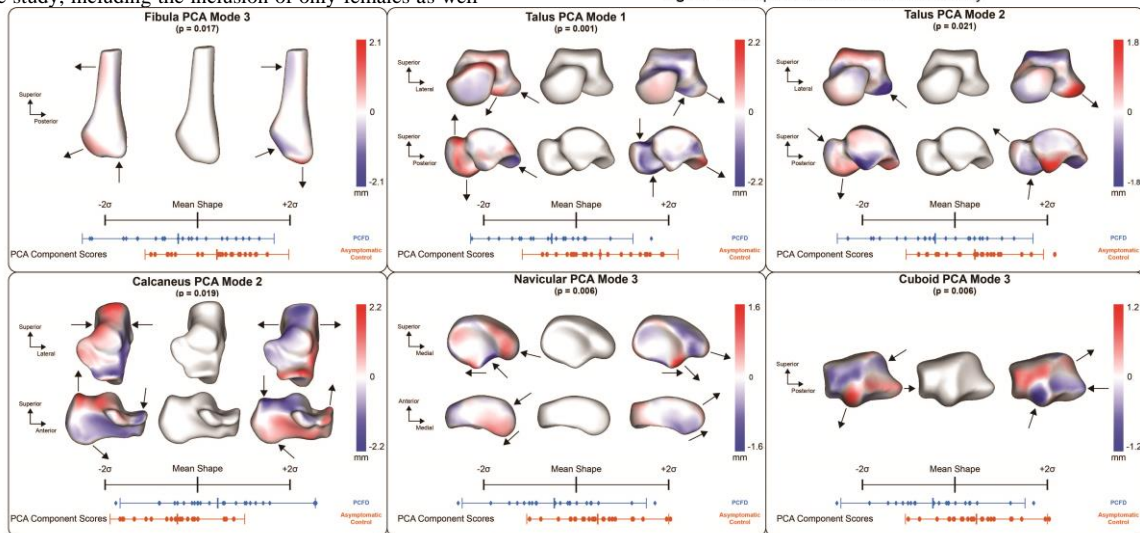


Figure 2: Quantitative visual description of significant PCA modes. Bone shape variations (mean and  $\pm 2$  standard deviations) and P-values for each mode represent a group-wise comparison of the PCA component scores for the indicated mode. Arrows indicate focal locations of morphological differences/changes across the mode.